2014 IEEE International Conference on Robotics & Automation (ICRA)
Hong Kong Convention and Exhibition Center
May 31 - June 7, 2014. Hong Kong, China

Sensors for Micro Bio Robots via Synthetic Biology

Edward B. Steager[1], Denise Wong[1], Deepak Mishra[2], Ron Weiss[2]and Vijay Kumar[1]

***Abstract*— Microscale robots offer an unprecedented opportunity to perform tasks at resolutions approaching 1 μm, but the great majority of research to this point focuses on actuation and control. Potential applications for microrobots can be considerably expanded by integrating sensing, signal processing and feedback into the system. In this work, we demonstrate that technologies from the field of synthetic biology may be directly integrated into microrobotic systems to create cell-based programmable mobile sensors, with signal processors and memory units. Specifically, we integrate genetically engineered, ultraviolet light-sensing bacteria with magnetic microrobots, creating the first controllable biological microrobot that is capable of exploring, recording and reporting on the state of the microscale environment. We demonstrate two proof-of-concept prototypes: (a) an integrated microrobot platform that is able to sense biochemical signals, and (b) a microrobot platform that is able to deploy biosensor payloads to monitor biochemical signals, both in a biological environment. These results have important implications for integrated micro-bio-robotic systems for applications in biological engineering and research.**

I. Introduction

Rapid fundamental progress in microrobotics has given rise to opportunities for new applications. Due to the similarity in length scale to single cells, microrobots enable the investigation of microbiology in ways which were not previously possible. Examples include manipulating and arranging single cells [1], [2], probing interactions with cells [3], [4], and cell surgery [5]. Cells have also been used for propulsion and control of microrobots. For instance, *Serratia marcescens* has been examined as an effective actuator for propelling microbeads and micro fabricated plates, and swarms of magnetotactic bacteria have been employed for delivering small payloads [6], [7], [8]. Alternatively, the natural environmental responses of cells have been used in motility-based biosensors, where readout is performed based on the motility of the cells [9].

Concurrently, rapid advancements in synthetic biology have enabled the design of cells with highly specified functionality through genetic engineering [10]. Cells are compelling candidates for use in micro scale systems for two particular reasons. Firstly, biological cells are self-contained systems which do not need an external power source. Secondly, they have the natural ability to respond to environmental cues, such as changes in chemical concentration, light exposure, and even magnetic field orientation. This sensory framework is contained in an exquisitely small package, which in the case of the rod-shaped bacteria *Escherichia coli* is typically 1 μm in diameter and 2 μm in length. Given the extensive knowledge base on the genetic and proteomic makeup of model organisms such as *E.coli*, as well as rapid advances in genetic engineering, we can extend the idea of cells being good natural candidates for microscale biosensors to the concept of these cells being *programmable*. This programmability can be extended well beyond innate sensing capabilities. For example, synthetic gene networks have been designed to create digital signal processing capabilities such as cell-based memory units, data-loggers, counters, edge detectors, and multi-input logic circuits as well as analog processing functions such as filtering and timing [11], [12], [13], [14], [15], [16]. Furthermore, by employing existing mechanisms for quorum-sensing that enable communication between cells, capabilities can be extended to include population-level sensing and decision making [17]. Combining advancements in both microrobotics and synthetic biology is an investigative path with significant potential [18].

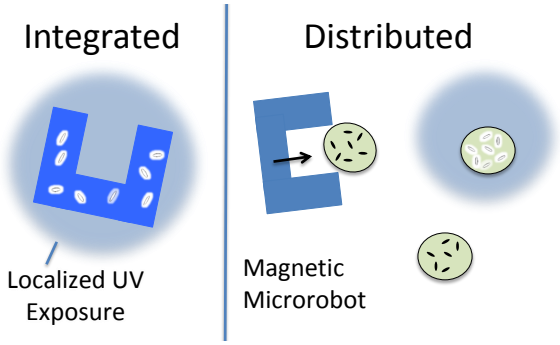

Fig. 1. Biosensors. Cells engineered to sense UV radiation are attached either directly to the Integrated magnetic microrobot (left), or attached to Distributed passive microplates (right). The integrated approach is useful for rapid exploration of a workspace, but cell response and readout is on the order of hours. The distributed approach requires arrangement of several passive sensors, but mapping can be performed more quickly due to greater coverage.

In this work, we demonstrate a microrobotic system capable of sensing environmental changes with spatial resolutions at the scale of individual cells. We combine two technologies: (a) the ability to create mobile microrobots using magnetic actuation; and (b) tools from synthetic biology to create novel biosensors. These biosensors are designed to sense low doses of ultraviolet (UV) light. The information is stored in a *toggle switch* architecture —- a switch that allows cells to toggle between stable states based on environmental stimuli —- and the information readout is performed via production of fluorescent proteins within the cell. This form of sensing is useful for seeking potentially pathological conditions. The

[1] GRASP Laboratory, School of Engineering and Applied Sciences, University of Pennsylvania, Philadelphia, PA 19104, U.S.A. esteager, denwong, kumar@seas.upenn.edu
[2] Synthetic Biology Center, Massachusetts Institute of Technology, Cambridge, MA 02139 dmishra, rweiss@mit.edu

UV sensor is used here as a proxy for chemical biosensors, since it is simpler for proof-of-concept demonstrations with UV light, and, because of the similarity in architecture, it is not too difficult to engineer similar cells that can sense biochemicals.

We investigate two methodologies (Figure 1) for microrobotic biosensing systems. The first method, which we refer to as an integrated system, utilizes cells directly attached to magnetic microrobots. The integrated system enables rapid exploration of a region, however, biosensor readout takes considerably longer than actuation time. Thus, actuation time is greatly restricted by readout. In the second method, which we call a distributed system, we attach cells to microscale plates that are then independently arranged by a single magnetic robot. In this system, several biosensors are rapidly arranged to cover a region. In both systems, the sensor consists of a population of cells, whether they are attached to the microrobot or the passive microscale plate. A single cell is not a reliable biosensor because individual cells exhibit stochastic behavior. However, reliable results can be obtained for groups of cells. Fluorescence microscopy is used to read out the response of cell populations. Specifically, we show in this paper how sensors can be transported and read out to indicate the presence of UV radiation.

II. Methods

A. Experimental Setup

The experimental setup consists of four in-plane electromagnetic coils which use magnetic field gradients to actuate the magnetic microrobots. The coils are integrated on the stage of an epifluorescence microscope. The precise details of the setup have been previous described in detail and modeled [2].

B. Microrobot Fabrication

Microrobots are fabricated in a single-exposure process using traditional microfabrication techniques [1]. First a layer of 10% dextran in spin-coated on a clean glass slide, which acts as a sacrificial release layer. Next, a 2 μm layer of SU8-2002 is spin-coated. This layer is necessary as a mediating interface and enables uniform coating in the subsequent spin-coating step. Next, SU8 mixed with 5% iron oxide nanoparticles is spin-coated to a thickness in the range of 4-10 μm. A dark-field photomask is used during the exposure step, and the entire slide is then developed in PGMEA and dried with nitrogen.

C. Fabrication of Plasmids and Strains

Plasmids pHPTa and pCIRa were derived from the published pTAK plasmids and pZ expression vectors and previously published [11]. The plasmid pLPTa was built by performing site-directed mutagenesis on pHPTa to change the Glutamine at residue 233 of the cI protein to a Lysine to confer more sensitivity to UV irradiation. Co-transformations of pLPTa and pCIRa into $E.coli$ strain JM2.300 yielded the experimental strain for all data collection. The experimental strains were cultured at 37°C in LB broth (BD Biosciences) supplemented with appropriate levels of ampicillin and tetracycline (Sigma) to maintain selection. Typically, cultures were inoculated with appropriate selection antibiotics and initial isopropyl-beta-thiogalactopyranoside (IPTG) to set toggle state and grown at 37°C for 16 hours. Cells were centrifuged and resuspended in fresh LB broth twice before additional growth periods dependent on downstream experiments.

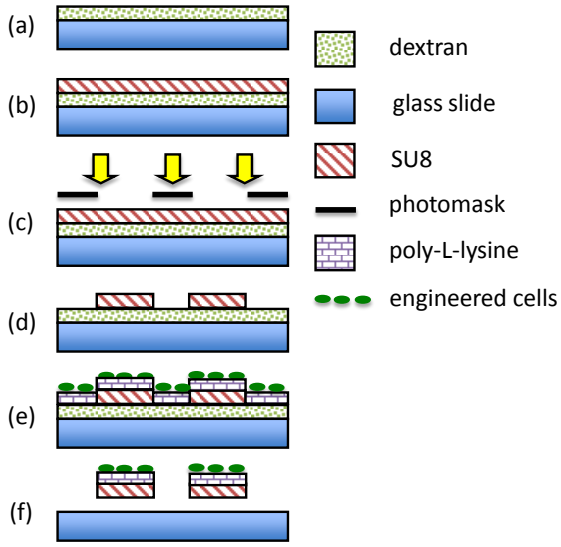

Fig. 2. Biosensor Microfabrication. (a) Glass slides are coated with dextran, which acts as a water-soluble sacrificial release layer. (b) SU8 forms the substrate of the biosensor. (c-d) Biosensors are patterned with photolithography. (e) Poly-L-lysine is deposited on the biosensor surface to enhance attachment of cells. (f) Microrobots are released in solution and dextran dissolves.

D. Fabrication of Biosensors

Biosensors are SU8 epoxy microstructures with bacteria adhered to the surface (Figure 2). The fabrication process is optimized for compatibility with biological cells as well as compatibility with traditional bright-field and fluorescence microscopy. Initially, a water-soluble sacrificial layer of dextran is spin-coated onto a No. 0 glass slide to allow release of biosensors in subsequent experimental steps. On top of the dextran layer, 5-10 μm thick SU8 2000 series negative tone, photosensitive epoxy plates are fabricated using a single exposure through a chrome mask. For this study, a combination of 40, 60 and 80 μm diameter disks were fabricated. $E.coli$ cells do not naturally adhere to SU8, so the surface of the plates were treated with 0.1% poly-L-lysine for 10 minutes, a protein which promotes binding of biological cells. The slides were then dried with compressed air. For SU8 experiments, following overnight cultures and subsequent washing away of IPTG, cells were grown in liquid LB media supplemented with appropriate antibiotics at 37°C for 4 hours before being deposited onto poly-L-lysine substrates and allowed to adhere for 5-10 minutes. Excess cells were washed from the surface and biosensors released into the experimental setup by inversion. Integrated biosensors were treated in a similar manner.

E. Flow Cytometry

Flow cytometry is used to characterize the level of fluorescence of individual cells. For cytometry experiments, following overnight cultures and subsequent washing away of IPTG, cells were grown in liquid culture at 30°C for 2 hours before exposure to UV irradiation (Stratalinker UV Crosslinker 2300) and additional growth at 30°C for 6 hours before analysis using a LSRFortessa cell analyzer (BD Biosciences) equipped with 488-nm argon excitation laser and 530/15 nm emission filter and a PMT setting of 360 V. Measurements were calibrated using Rainbow Calibration Particles (Spherotech RCP-30-5A) to normalize data between different experimental runs. For each sample, 10,000 events were collected.

F. Microscopy and Tracking

Integrated and distributed biosensors were actuated and positioned using bright-field microscopy. Readout was performed using fluorescence at excitation/emission wavelengths optimized for green fluorescence protein (GFP). Although SU8 epoxy is fluorescent at wavelengths close to GFP, the emission spectra of SU8 and GFP do not significantly overlap.

G. UV Exposure

Cells were exposed to UV light with a mercury lamp with collimation optics. The light source was masked to create discrete regions of UV exposure. Exposure times of 10 seconds were sufficient to induce the population to switch to high state, thus activating the synthetically engineered response of producing Green Fluorescent Protein (GFP), which is a readout for this high state.

III. Low Power Toggle Cells

A. Biochemical Model

Bistability occurs in a genetic circuit when two repressible promoters are arranged in a mutually inhibitory network [11]. Promoters regulate the activity of genes that transcribe proteins. Each promoter, pλ and plac, triggers a gene, lacI and λcI respectively, that regulates the production of a protein, LacR and λCI respectively, which represses the behavior of the other promoter, Figure 3. In the absence of inducers, two stable states are possible: (1) when promoter, plac, transcribes the repressor protein λCI (low-state,) (2) when promoter, pλ, transcribes the repressor protein LacR (high-state.) A transient, externally triggered inducer can be used to switch between these two stable states. Hence the name toggle switch. In this toggle switch, the inducers are chemical inducer IPTG and UV light.

By inducing the cells with IPTG, the transcription of protein LacR is repressed, which results in a high level of activity of gene λcI and the transcription of protein λCI (low-state), Figure 3(b). At low-state promoter pλ is repressed and therefore the activity of gene lacI is low. The cells will stay in low state even after IPTG is removed from the environment Figure 3(c). By inducing the cells with a transient pulse of UV light, the cell switches to high-state. UV light

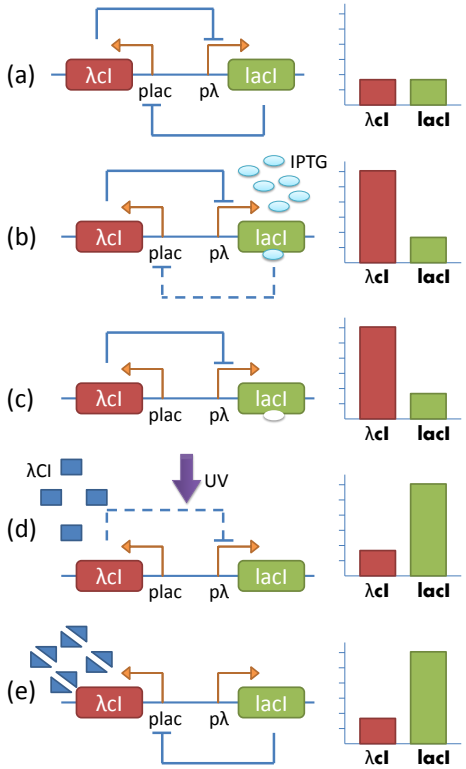

Fig. 3. Schematic showing gene circuit under different inducers and the corresponding activity of genes λcI and lacI. (a) No inducer, basal levels of activity of both genes, (b) Induction with IPTG reduces activity of lacI and increases activity of λcI, (c) Low-state, even after IPTG is removed the cell is stable in low-state, (d) Induction with UV light causes the degradation of protein λCI and increases activity of lacI, and is linked to GFP production (e) High-state, even after the UV light is removed the cell is stable in high-state.

causes repairable DNA-damage wherein the DNA becomes single-stranded, this activates an SOS-pathway and causes degradation of the protein λCI Figure 3(d). The degradation of protein λCI alleviates the repression of promoter pλ, increases the activity of gene lacI and hence the transcription of protein LacR. This protein represses the promoter plac and therefore the activity of gene λcI is low, Figure 3(e). In order to detect that a cell is at high state, transcription of green fluorescent protein (GFP) is synthetically engineered to be triggered by the transcription of the protein LacR. Thus, GFP transcription occurs in parallel with LacR transcription and is used as a signal indicating a cell is at high-state during experiments.

While bistable systems occurs naturally in biology, most are difficult to interface with as the inducers are not easily controlled externally and states are difficult to determine externally as well. The specific sensor cell used in the experiments described here are *E.coli* JM2.300 cells synthetically engineered to include plasmids pLPTa and pCIRa. Plasmids are circular DNA molecules separate from the chromosomal DNA within the cell that carries a few genes that can be expressed within the cell. Plasmid pCIRa carries the genes for GFP production which is used as a reporter for high-state[19]. Plasmid pLPT is the regulatory circuit that contains the genes λcI and lacI and controls the expression of GFP in plasmid pCIRa.

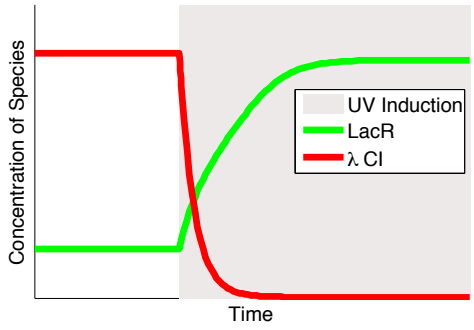

Fig. 4. Mathematical model of the toggle switch dynamics. Transition between low-state where protein λCI is abundant and represses the transcription of protein LacR and high-state when protein LacR is abundant and represses the transcription of protein λCI. The time scale for the case in this work is on the order of hours.

B. Mathematical Model

The interactions between the components in the genetic toggle circuit can be described by a pair of coupled dimensionless nonlinear differential equations [11]:

$$\frac{dU}{dt} = \frac{\alpha_1}{1+V^{\beta}} \quad U \ , \ \frac{dV}{dt} = \frac{\alpha_2}{1+U^{\gamma}} \quad V$$

where U is the concentration of repressor protein LacR, V is the concentration of repressor protein λCI, α_1 is the effective rate of synthesis of repressor protein LacR, α_2 is the effective rate of synthesis of repressor protein λCI, β is the cooperativity of repression of promoter pλ and γ is the cooperativity of promoter plac.

Figure 4 illustrates the interactions between levels of proteins λCI and LacR. The start of the graph shows the cell in low-state after IPTG induction when the level of protein λCI is high and level of protein LacR is low. The grey region indicates UV induction, this is modeled by decreasing the effective rate of synthesis of repressor protein λCI, α_2, and decreasing the cooperativity of repression of promoter, pλ. Increasing the effective rate of synthesis of repressor protein LacR, α_1, has a similar effect. UV induction causes a sharp change in the levels of each protein which destabilizes the high λCI state and drives the system to switch to the other stable state where the level of protein λCI is low and the level of protein LacR is high and as a result GFP is expressed. While the UV light exposure is transient, the effects of the induction are lasting and therefore the induction process extends beyond the duration of the UV light exposure.

Stochasticity in this system arises from the combination of bistable architecture with bimolecular processes involving few molecules [20]. This results in bimodal population distributions despite the same experimental conditions and induction levels. It has been shown that even a single-molecule event may trigger such phenotype switching [21]. Therefore, reading the fluorescence signal from multiple cells is important.

C. Cell Validation

Engineered cells need to be designed, tested and verified in liquid or agar cultures before integrating them with microrobots and sensor plates. Cells in JM2.300 background harboring both plasmids pCIRa and pLPTa as described in

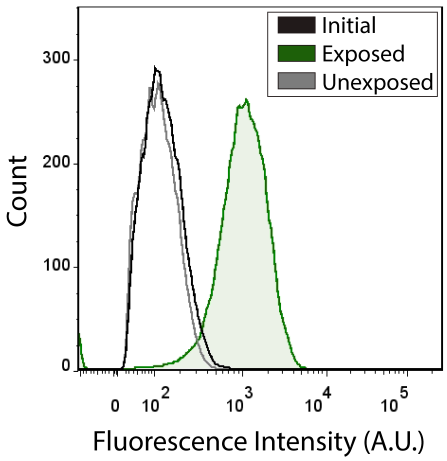

Fig. 5. Flow cytometry analysis of engineered bacterial cells. Cells in JM2.300 background harboring both pCIRa and pLPTa exposed to 50 μJ/cm^2 UV irradiation. Initially, a homogenous population shows basal levels of fluorescence (black). The split population is then given or not given UV input and monitored after 6 hours with the exposed cells having a median fluorescence of 1030 A.U. and unexposed cells having a median fluorescence of 106 A.U., an approximately 10-fold increase in GFP fluorescence.

the methods were first tested and analyzed in a robot-free environment. Bulk cultures of the genetically engineered cells were grown to stationary phase over 16 hours at 37°C in the presence of IPTG. The introduction of IPTG set the cells into a state of high cI and low LacR with a basal level of GFP fluorescence. The IPTG was subsequently washed out and cells were grown in exponential phase for 3-4 cell divisions (2 hours at 30°C). The culture was split into two aliquots, and one was exposed to 50 μJ/cm^2 UV irradiation. The two independent cultures were then grown for an additional 9-12 cell divisions (6 hours at 30°C) and analyzed by flow cytometry. For cells exposed to UV irradiation compared to cells that did not receive any UV irradiation, there is an approximately 10-fold increase of fluorescence in the GFP channel (Figure 5).

IV. Results and Discussion

A. Biosensor Transport

Biosensors are pushed in fluid using a magnetic robot (Figure 6). The sensor height should be a minimum of 5 μm so that the magnetic microrobot properly engages the edge of the biosensor for positioning. Microrobots transport 40-80 μm diameter biosensors of all sizes at speeds ranging from 0 to roughly 10 μm/s, despite the relatively significant viscous shear between the disk-shaped biosensor and the substrate. This process may be performed autonomously using visual feedback, as demonstrated in previous work [2].

B. Sensor Response

To replicate the appropriate cellular response after transferring cells between labs, as well as to characterize the UV response on the experimental apparatus used for magnetic actuation, cells were again characterized for UV exposure dose in liquid culture. The response is dramatic for UV exposure times of approximately 10 s as observed using fluorescence microscopy (Figure 7). It should be noted that

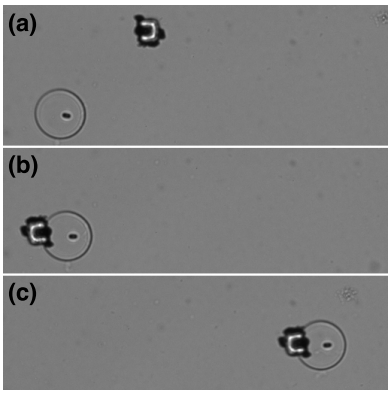

Fig. 6. Transport of biosensor substrates. (a-c) An 80 μm SU8 plate is approached from the left, engaged, and transported. Biosensors are individually distributed in this fashion.

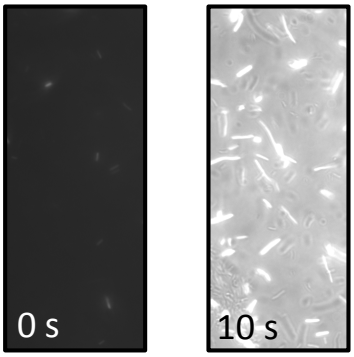

Fig. 7. Low power toggle cells in low vs high states at 40$\times$ magnification. (Left) With no exposure to UV, the bulk of the population of cells stay remain in the low state (non fluorescent), however a small number of cells do express GFP. (Right) 10 s exposure to UV light induces cells to switch to high state, thus expressing GFP, but the expression of sufficient fluorescence for read out takes several hours. The high state image is taken 12 hours after exposure (induction).

exposure times much greater than 10 s cause cell death, which is an expected outcome. It was not assumed that cells would respond as designed upon attachment to biosensors. The attachment of cells to substrates or to the poly-L-lysine interface was anticipated to be a potential disruption to proper operation of the designed circuit. However, the cellular response is largely preserved for the conditions of the experiment. We did find that exposure conditions were affected by experimental apparatus. Microscope optics and lab ware such as Petri dish lids act as filters at the UV wavelengths that trigger the toggle switch.

As shown in Figures 8 and 9, GFP response is strong after 12 hrs, although not all cells switch to high state, which is observed as fluorescence. Even in an unexposed population of cells, there is a small subpopulation of cells in high state. Therefore, larger sensors give a more reliable readout of UV exposure due to the larger number of attached cells. The smallest sensors only have a few high state cells for the cell densities achieved in these experiments, and it should be considered that there is a significant chance that readings from small sets of total cells (5-10) may result in incorrect determination of UV exposure.

For the integrated system, where low power toggle cells

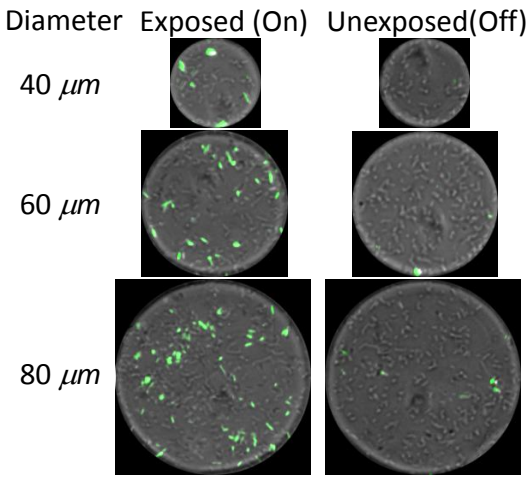

Fig. 8. Sensor readout. Exposed sensors exhibit higher mean fluorescence with significantly higher numbers of cells in high state. Unexposed sensors still include a small population of fluorescing cells, which is an example of biological stochasticity. Thus, larger sensors give more reliable readout due to the higher number of cells.

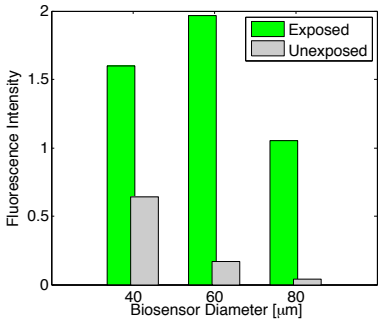

Fig. 9. Mean fluorescence intensity averaged across several distributed sensor micro plates. Exposed sensors have significantly higher mean fluorescence intensity in comparison to unexposed sensors.

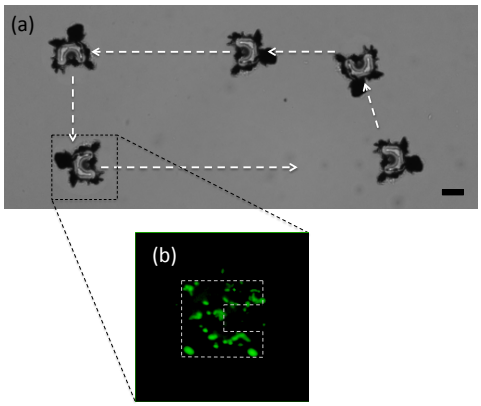

Fig. 10. Integrated biosensing microrobots. (a) Magnetic microrobots are driven through a region of interest. Scale bar is 40 μm. (b) Cells attached in high state. Robot outline is indicated by dashed lines.

are directly attached to the microrobot, a workspace may be traversed in a matter of seconds (Figure 10). However, expression of fluorescence takes several hours after exposure to UV light. Thus, mapping spatial location to the region of UV exposure is ambiguous, unless the robot is moved on a time scale matching readout. For the distributed system, collection and arrangement of biosensors takes minutes, and

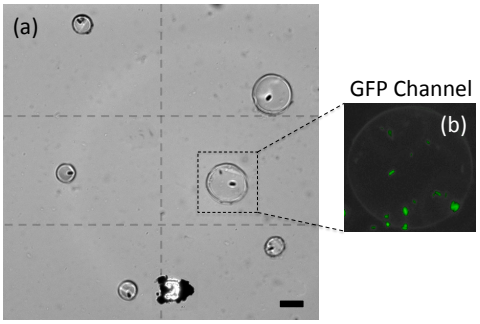

Fig. 11. Distributed biosensors. (a) Six sensors are distributed to cover six division of a workspace, as delineated with dashed gray lines. (b) High state cells attached to the sampled biosensor indicate exposure to UV light. Scale bar is 40 μm.

the position of the sensors are spatially correlated with UV exposure. As shown in Figure 11, distributed biosensors are collected and arranged with the microrobot so that six divisions of the workspace are occupied by sensors. Current work in synthetic biology is targeted at greatly reducing the time required for readout, which would greatly enhance the practicality of these systems.

V. Conclusion

In this paper, we demonstrated the integration of microrobotic actuation techniques with engineered cells to create mobile biosensors. For this proof-of-concept prototype, we used cells that were programmed to respond to and report on exposure to UV light. This is the first time low power toggle cells have been attached as biosensors on to robots, a significant achievement that promises a pathway for transitioning research in synthetic biology to robotics. This means that cells that can serve as chemical sensors, data-loggers, or quorum sensors can also be incorporated into such systems. Thus advances in synthetic biology offer many techniques to integrate new capabilities into cells and microrobots, and provide an alternative path to microfabricating organic signal processors, power sources, and memory units.

While the results of this study are promising and suggest many exciting bridges between synthetic biology and robotics, there are several practical considerations. In most conventional robotic systems the characteristic time scales for sensing, processing and actuation are matched allowing for closed loop feedback control and motion planning. In our prototype systems, biosensors prove to be the bottleneck. The characteristic time for genetic regulation is of the order of minutes and that for cell division is of the order of tens of minutes. However, as seen in Figure 11, it is clear that a single robot can be used to place tens or even hundreds of sensors in targeted location enabling cell-specific measurements in samples of biological tissue. This points to an exciting direction for future research.

Acknowledgment

We gratefully acknowledge the support of ONR grants N00014-07-1-0829 and N00014-11-1-0725, and the UPS Foundation.

References

[1] M. S. Sakar, E. B. Steager, D. H. Kim, M. J. Kim, G. J. Pappas, and V. Kumar, "Single cell manipulation using ferromagnetic composite microtransporters," *Applied Physics Letters*, vol. 96, p. 043705, 2010.

[2] E. B. Steager, M. S. Sakar, C. Magee, M. Kennedy, A. Cowley, and V. Kumar, "Automated biomanipulation of single cells using magnetic microrobots," *The International Journal of Robotics Research*, vol. 32, no. 3, pp. 346–359, 2013.

[3] M. Sakar, S. Schurle, S. Erni, F. Ullrich, J. Pokki, D. Frutiger, O. Ergeneman, B. Kratochvil, and B. Nelson, "Non-contact, 3d magnetic biomanipulation for in vivo and in vitro applications," in *Optomechatronic Technologies (ISOT), 2012 International Symposium on*. IEEE, 2012, pp. 1–2.

[4] E. B. Steager, B. Zerne, M. S. Sakar, V. Muzykantov, and V. Kumar, "Assessment of protein binding with magnetic microrobots in fluid," in *IEEE International Conference on Robotics and Automation*, 2013.

[5] L. Feng, M. Hagiwara, A. Ichikawa, and F. Arai, "On-chip enucleation of bovine oocytes using microrobot-assisted flow-speed control," *Micromachines*, vol. 4, no. 2, pp. 272–285, 2013.

[6] S. Martel, C. Tremblay, S. Ngakeng, and G. Langlois, "Controlled manipulation and actuation of micro-objects with magnetotactic bacteria," *Applied Physics Letters*, vol. 89, 2006.

[7] B. Behkam and M. Sitti, "Bacterial flagella-based propulsion and on/off motion control of microscale objects," *Applied Physics Letters*, vol. 90, 2007.

[8] M. S. Sakar, E. B. Steager, D. H. Kim, A. A. Julius, M. J. Kim, V. Kumar, and G. J. Pappas, "Modeling, control and experimental characterization of microbiorobots," *International Journal of Robotics Research*, vol. 30, pp. 647–658, 2011.

[9] E. B. Steager, M. S. Sakar, D. H. Kim, V. Kumar, G. J. Pappas, and M. J. Kim, "Electrokinetic and optical control of bacterial microrobots," *Journal of Micromechanics and Microengineering*, vol. 21, p. 035001, 2011.

[10] P. E. Purnick and R. Weiss, "The second wave of synthetic biology: from modules to systems," *Nature Reviews Molecular Cell Biology*, vol. 10, no. 6, pp. 410–422, 2009.

[11] T. S. Gardner, C. R. Cantor, and J. J. Collins, "Construction of a genetic toggle switch in Escherichia coli," *Nature*, vol. 403, pp. 339–342, 2000.

[12] K. Rinaudo, L. Bleris, R. Maddamsetti, S. Subramanian, R. Weiss, and Y. Benenson, "A universal rnai-based logic evaluator that operates in mammalian cells," *Nature biotechnology*, vol. 25, no. 7, pp. 795–801, 2007.

[13] A. E. Friedland, T. K. Lu, X. Wang, D. Shi, G. Church, and J. J. Collins, "Synthetic gene networks that count," *science*, vol. 324, no. 5931, pp. 1199–1202, 2009.

[14] J. J. Tabor, H. M. Salis, Z. B. Simpson, A. A. Chevalier, A. Levskaya, E. M. Marcotte, C. A. Voigt, and A. D. Ellington, "A synthetic genetic edge detection program," *Cell*, vol. 137, no. 7, pp. 1272–1281, 2009.

[15] T. K. Lu, A. S. Khalil, and J. J. Collins, "Next-generation synthetic gene networks," *Nature biotechnology*, vol. 27, no. 12, pp. 1139–1150, 2009.

[16] T. Ellis, X. Wang, and J. J. Collins, "Diversity-based, model-guided construction of synthetic gene networks with predicted functions," *Nature biotechnology*, vol. 27, no. 5, pp. 465–471, 2009.

[17] L. Weiss, J. Badalamenti, L. Weaver, A. Tascone, P. Weiss, T. Richard, and P. Cirino, "Engineering motility as a phenotypic response to luxi/r-dependent quorum sensing in escherichia coli," *Biotechnology and Bionengineering*, vol. 100, pp. 1251–1255, 2008.

[18] M. S. Sakar, E. B. Steager, D. H. Kim, A. A. Julius, M. J. Kim, V. Kumar, and G. J. Pappas, "Biosensing and actuation for microbiorobots," in *IEEE International Conference on Robotics and Automation*, Anchorage, AL, 2010, pp. 3141–3146.

[19] H. Kobayashi, M. Kærn, M. Araki, K. Chung, T. S. Gardner, C. R. Cantor, and J. J. Collins, "Programmable cells: interfacing natural and engineered gene networks," *Proceedings of the National Academy of Sciences of the United States of America*, vol. 101, no. 22, pp. 8414–8419, 2004.

[20] A. Novick and M. Weiner, "Enzyme induction as an all-or-none phenomenon," *Proceedings of the National Academy of Sciences*, vol. 43, pp. 553–566, 1957.

[21] P. J. Choi, L. Cai, K. Frieda, and X. S. Xie, "A stochastic single-molecule event triggers phenotype switching of a bacterial cell," *Science*, vol. 322, p. 442, 2008.